IEEE Access
Multidisciplinary ⋮ Rapid Review ⋮ Open Access Journal

Received 21 May 2024, accepted 10 June 2024, date of publication 14 June 2024, date of current version 9 July 2024.

Digital Object Identifier 10.1109/ACCESS.2024.3414603

RESEARCH ARTICLE

A Distributed Consensus-Based Optimal Dispatch Control Strategy for Hybrid AC/DC Microgrids

MUHAMMAD SALMAN[1,2], YANJUN LI[3], AND JI XIANG[1,2], (Senior Member, IEEE)
[1]College of Electrical Engineering, Zhejiang University, Hangzhou 310027, China
[2]Huzhou Institute of Zhejiang University, Huzhou 313000, China
[3]School of Information and Electrical Engineering, Hangzhou City University, Hangzhou 310015, China

Corresponding authors: Ji Xiang (jxiang@zju.edu.cn) and Yanjun Li (liyanjun@zucc.edu.cn)

This work was supported in part by the National Natural Science Foundation of China under Grant 62073290 and Grant 62173295.

ABSTRACT This paper proposes a consensus-based distributed control strategy for optimal power dispatch, frequency control, and DC voltage regulation in islanded hybrid AC/DC microgrids (HMGs). For the primary control, local control of AC/DC DGs is implemented using the droop-based control. Regarding the secondary control, a coordination-based distributed optimal control approach is initially introduced. Subsequently, control objectives, including AC frequency restoration, DC voltage regulation, and optimal economic operation of all participating AC/DC DGs with power limit consideration in the hybrid AC/DC microgrid, are achieved based on the proposed optimal consensus based controller. Moreover, the proposed controller integrates frequency regulation with optimal dispatch, reactive marginal dispatch with voltage regulation in AC microgrid (MG), and optimal dispatch with voltage regulation in DC MG, all at the secondary control level, eliminating the need for a tertiary controller. Furthermore, a distributed active power control method is proposed for managing multiple bi-directional interlinking converters (BICs), ensuring proportional active power sharing for BICs to prevent overloading. Extensive simulations are conducted using MATLAB/Simulink to showcase the effectiveness of the suggested coordination-based control.

INDEX TERMS Distributed control, economic dispatch (ED), hybrid AC/DC microgrids (HMGs), multi-objective control, secondary control.

NOMENCLATURE

INDEXES

DG	Distributed generation.
BIC	Bidirectional interlinking converter.
HMGs	Hybrid AC/DC micorgrids.
ILCs	Interlinking converters.
ESSs	Energy storage systems.
MGs	Microgrids.
PnP	Plug-and-play.
PI	Proportional-integral.
AC	Alternating current.
DC	Direct current.
RESs	Renewable energy sources.
ED	Economic dispatch.
DMPC	Distributed model predictive control.
IC	Incremental cost.
RMC	Reactive marginal cost.
GOP	Global economic operation.

VARIABLES

ω, ω^*	Output and nominal frequency.
P, ϕ_Q	Actual active power and RMC.
k_{d_P}, k_{d_q}	Droop coefficients.
V_{isec}	Secondary voltage reference.
E	Output voltage.
C_i	DG_i generation cost.
P_i	Output power of DG_i.
a_i, b_i, c_i	Cost coefficients of DG_i.
λ_{pi}	Incremental cost of AC_{DGi}.
γ_{pi}	Incremental cost of DC_{DGi}.
P_i, Q_i, V_i	Output active, reactive power and voltage.
V_{refi}	reference voltage for DG_i.
λ_{refi}	Optimal incremental cost.
P_{refi}	Optimal power generated by DG_i.
φ_j	Consensus index for AC voltage sharing proportion.
m	DC droop coefficient.
γ_{dc}	Measured DC IC.
ϵ_j	DC voltage sharing proportion.
V_{min}, V_{max}	J^{th} DG minimum and maximum voltage.

The associate editor coordinating the review of this manuscript and approving it for publication was Hao Wang.

P_{LF}	Load factor of AC/DC DGs and BICs.
$T(s)$	PI controller for voltage loop.
$J(s)$	PI controller for AC reactive power and DC IC loop.
$\delta_{p(j)}$	Load factors of BIC.
ϱ_{P-refi}	Control reference of i^{th} BIC.
τ, μ	Secondary control reference power signal for BIC.
P_{LF}	Load factor of AC/DC DGs.
$e_{BIC,j}$	Error in power sharing between BICs.

I. INTRODUCTION

The Hybrid Microgrid (HMG) represents an innovative, cutting-edge solution for power distribution, providing the adaptability to easily include several kinds of both AC and DC energy storage systems (ESSs), distributed generators (DGs), and renewable energy sources (RESs) [1]. Lately, noticeable attention has been paid to investigating hybrid AC/DC microgrids. This heightened interest stems from the unique capability of HMGs to streamline and optimize the integration of AC and DC generations, loads, and energy storage systems within a single electrical infrastructure [2]. Usually, a hybrid AC/DC microgrid consists of both an AC and a DC microgrid (MG), connected via a single or multiple interlinking converters (ILCs). Figure 1 depicts a typical hybrid AC/DC HMG configuration comprising an AC and DC and multiple bi-directional Inverters (BICs) operating in parallel. Due to their unique generating properties, different DGs— AC and DC, usually have varied generation costs. Consequently, establishing a cost-efficient strategy and optimal solution for the HMG system becomes imperative [3]. Therefore, employing suitable DG dispatch method is essential to optimize the total generation cost (TGC).

Hierarchical control, encompassing primary, secondary, and tertiary control, has been extensively employed in governing AC and DC Microgrids [4]. For primary control, droop control methods are commonly employed to regulate the frequency or voltage of DGs within AC/DC sub-grids [5]. Similarly, in BICs, droop control methods are utilized to govern the power transmission among AC and DC sub-grids [6]. Nevertheless, the droop control method faces limitations in addressing steady-state frequency and voltage deviations and precise power dispatch requirements.

In MGs, inside the three-tier hierarchical control structure, each tier operates at distinct time scales [4]. The primary level, the quickest among the three, focuses on upholding MG stability and ensuring equitable power distribution [7]. Following this, the secondary tier rectifies alterations made by the primary control level [2]. Lastly, the tertiary tier, operating at the slowest pace, concentrates on economic dispatch, striving for the most cost-effective energy generation while harmonizing with the main grid [8]. However, isolated MGs are susceptible to rapid fluctuations in generation

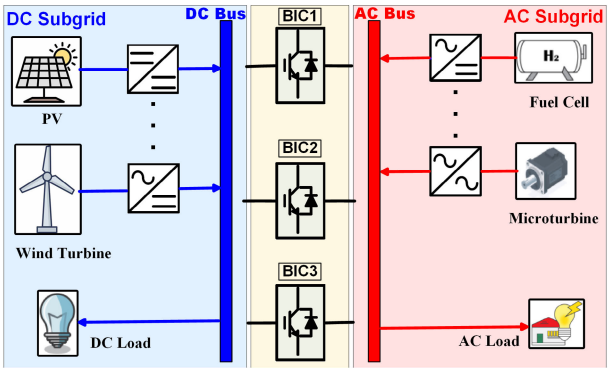

FIGURE 1. Architecture of hybrid AC/DC microgrid.

and demand, which the tertiary control level struggles to promptly address. Recent studies advocate for aligning the time scale of tertiary control with that of the secondary level to mitigate this issue. Additionally, the slower updating of power references from the tertiary level may lead to exceeding the power limits of DGs. It is possible to achieve economic dispatch, and restoration of voltage and frequency in MGs at the secondary control level through distributed consensus controllers that share their information to coordinate their control sequences. In this way, in addition to avoiding the need to have a controller for each objective, the overall performance of the microgrid is enhanced in terms of robustness and reliability. Recent studies on DC MGs [9], [10], AC MGs [11], [12], and HMGs [13] have highlighted that solitary MGs are vulnerable to rapid fluctuations in demand and generation. Consequently, for optimal dispatch to be effective, it should align with the secondary control level.

Regarding secondary control, economic dispatch (ED) control techniques can be grouped into three categories: centralized, decentralized, and distributed control, depending on their reliance on communication infrastructure [14]. Deploying centralized or decentralized controllers is not advisable for MGs with many DGs and BICs, i.e., implementing centralized controllers becomes impractical due to the excessive computational load and susceptibility to single-point failures [15], [16]. The problem with these centralized controls is the common point of failure in the communication network, making it vulnerable to disruptions. Additionally, it imposes a high computational burden due to the need for a single controller to manage all operations also scalability require changes in the control. Moreover, decentralized strategies for ED in MGs with cost-based droop do not integrate the secondary control loop [17], [18]. For decentralized controllers optimal solution is difficult to achieve.

In the previous few years, substantial efforts have been dedicated to research on the economic dispatch of HMGs. The authors in [19] incorporate the generation limits of the DGs into the centralized optimization problem. However, these controls are prone to single points of failure. As discussed

TABLE 1. Comparisons of different optimal control methods HMGs from the literature.

Ref.	Operation Principle	CM	FR	VR	PL	RPD	MBICs	Microgrid Structure
[21]	Distributed control	Yes	N/A	No	No	N/A	No	DC MG
[22]	Distributed control	No	N/A	Yes	N/A	N/A	No	DC MG
[23]	Distributed control	Yes	No	Yes	No	No	No	AC MG
[24]	Distributed control	Yes	No	Yes	No	No	No	AC MG
[25]	Distributed control	No	Yes	Yes	No	No	No	AC MG
[26] [27] [28]	Consensus-PI	Yes	No	No	Yes	No	No	HMG
[29]	Distributed control	Yes	No	No	Yes	No	No	HMG
[31]	Distributed control	No	Yes	Yes	No	No	No	HMG
[32]	DMPC	No	Yes	Yes	Yes	No	Yes	HMG
Proposed Control	Coordination-Based Control	Yes	Yes	Yes	Yes	Yes	Yes	HMG

CM: Cost Minimization; **VR**: Voltage Regulation; **RPD**: Reactive Power Dispatch; **FR**: Frequency Regulation; **PL**: Power limits; **MBICs**: Multiple BICs.

above the centralized controllers are mostly suitable for small MGs, also the scalability is requires changes in the control. In [20], the authors propose an integrated controller for ED, voltage, and frequency restoration. However, their proposal does not address the communication aspect of BICs. In [21], the authors proposed a distributed control aiming to regulate DC DGs voltage while considering ED within the DC MG. Similarly, in [22] the authors presented a distributed model-based cooperative control for isolated DC MGs. The proposed control achieved the objective of maintaining balanced voltage at each dc–dc buck converter in steady state, while maintain a stable synchronization in transient state. Conversely, [23] presents a multi-level control for AC MG to address the issue of frequency and ED. In [24], the feasibility of multi-level control in an AC MG is investigated. Additionally, [25] proposes a distributed approach to ensure frequency regulation and power sharing for AC DGs in AC MG. Nonetheless, the strategies outlined in [21], [22], [23], [24], and [25] are specifically tailored for individual AC or DC MGs, limiting their applicability to a single MG configuration.

Consensus-based schemes aimed at minimizing operational costs in HMGs have been presented in [26], [27], [28], and [29]. In [26] and [27], the authors presented a distributed ED control for hybrid microgrids, while in [28], a distributed hybrid MCSA-ADMM algorithm is proposed for HMGs. In [29], a consensus control for HMGs is suggested, but all the above controls failed in restoring variables altered by the droop control. The authors in [30] focused on the problem of distributed machine learning. A distributed control based on coordination-based control was suggested for HMGs in [31]. Accurate power sharing and restoration of variables were achieved, but the control failed to achieve cost minimization and use of multiple BICs. Similarly, in [32], the authors presented a distributed model predictive control (DMPC) for HMGs, which was related to proportional power sharing rather than economic dispatch.

Concerning the economic dispatch and distributed control of HMGs, existing methods typically exhibit one or more of the following primary problems: 1) Opting for a proportional load-sharing approach over an ED approach to effectively manage DGs within the HMG. 2) Execution of ED at the tertiary control level rather than the secondary level. 3) Lack of restoration for secondary variables such as AC frequency, DC bus voltage regulation, and under-utilization of multiple BICs. Moreover, current practices often focus solely on optimizing active power dispatch, neglecting reactive power dispatch. This oversight can lead to elevated operating expenses, given that the real power capacity is constrained. In order to remedy this, some of the apparent power capacity is allocated to producing reactive power.

A. STATEMENT OF CONTRIBUTION

To address the identified gaps, a distributed consensus-based secondary control technique for hybrid AC/DC is proposed to accomplish global economic operation (GOP) and optimal active and reactive power dispatch for all the participating AC/DC DGs. Similarly, a distributed normalized technique is proposed for the operation of multiple BICs to achieve normalized power sharing for multiple BICs under their power limits. Compared to existing control techniques, the distinctive features of the proposed control technique are recapitulated in Table 1. The contributions are listed below:

- A distributed optimal secondary control strategy for islanded hybrid AC/DC is proposed, which achieves seamless restoration of the variables (AC frequency and DC voltage) for the hybrid AC/DC microgrid while minimizing total operation cost. The proposed control is introduced at the secondary control level and achieves equal incremental costs (both active incremental cost (IC) and reactive marginal cost (RMC)) for all AC/DC DGs within their power limits in the HMG.
- A distributed normalized control is presented for the operation of multiple BICs, ensuring power sharing

among BICs based on their respective power capacities while adhering to their power limits.
- Finally, the proposed control exhibits robust performance w.r.t. other reported controls, effectively managing load changes and facilitating plug-and-play (PnP) operation.

B. ORGANIZATION

The rest of this paper is organized as follows: Section II offers a comprehensive background information on the optimal dispatch problem for hybrid AC/DC Microgrids. Section III outlines the proposed coordination-based distributed control for optimal dispatch in AC and DC sub-grids. Section IV details the overall control framework for HMG. In section V, comprehensive Matlab/Simulink tests and result are presented to validate the viability and efficacy of the suggested approach. Finally, the paper's conclusion is presented in Section VI.

II. CONSENSUS ALGORITHM AND ECONOMIC DISPATCH IN MICROGRIDS

A. GRAPH THEORY AND CONSENSUS ALGORITHM

Graph theory is widely employed in the examination of relationships among multiple objects. Graphs can be either undirected or directed, depending on whether the relationships between nodes are bidirectional or unidirectional. Each diagonal member of the degree matrix represents the number of edges connected to a particular node, or $[D]_{ij}$, which is a diagonal matrix. On the other hand, the adjacency matrix, denoted as $[A]_{ij}$, has zeros along its diagonal. The off-diagonal entries of $[A]_{ij}$ are assigned a value of 1 if node i has a connection with node j; else, they are assigned a value of 0. The adjacency term, a_{ij} is written as:

$$a_{ij}(t) = \begin{cases} 1 & \text{Data from DG}_j \text{ reaches DG}_i \text{ at } t \\ 0 & \text{Data from DG}_j \text{ cannot reach DG}_i \text{ at } t \\ 0 & j = i \end{cases} \tag{1}$$

The consensus algorithm entails each DG exchanging information with its neighboring DGs.

B. ACTIVE POWER DISPATCH

One of the main objectives in power dispatching within a Microgrid is to minimize the overall total generation cost (TGC) [33], often addressed through economic dispatch problem (EDP). The EDP is effectively tackled by calculating each AC or DC DG's active power contribution according to its cost features [17]. Factors such as fuel cost, maintenance cost, etc, which vary by DG type, are encompassed in the generation cost function. Generally, the cost function for EDP is represented as quadratic polynomials.

$$C_i(p_i) = a_i p_i^2 + b_i p_i + c_i, \tag{2}$$

where $C_i(p_i)$ represents DG_i generation cost, while, p_i is the output power of DG_i while a_i, b_i, c_i are the constant cost coefficients of the DG_i.

The aim of ED is to minimize the generation costs while accounting for the capacity constraints of the DGs. It can be formulated as follows:

$$\begin{cases} \min \sum_{i=1}^{n} C_i(p_i) \\ \sum_{i=1}^{n} p_i = p_{\text{load}} - p_{\text{loss}} \\ 0 \le p_i \le p_i^{\max} \end{cases} \tag{3}$$

where p_{load} is the total load power, p_{loss} is the power loss in power transmission, $p_i^{\max}$ is the maximum output power of DG_i, n denotes the number of DGs.

Then, the increments for AC and DC DGs in AC/DC MGs are given by:

$$\lambda_{pi} = \frac{dC(P_i)}{dP_i} = 2a_i P_i + b_i. \tag{4}$$

While for DGs in DC MG, we have,

$$\gamma_{pi} = \frac{dC(P_i)}{dP_i} = 2a_i P_i + b_i. \tag{5}$$

λ_i is supposed as the incremental cost (IC) of AC_{DGi}. While for the DC microgrid γ_i is assumed as the IC of DC_{DGi}. The power limits for the DGs in AC MG is given by:

$$\lambda_{\text{P}} = \begin{cases} 2\,a_i P_i^{\min} + b_i, P_i < P_i^{\min} \\ 2\,a_i P_i + b_i, P_i^{\min} < P_i < P_i^{\max} \\ 2\,a_i P_i^{\max} + b_i, P_i > P_i^{\max} \end{cases} \tag{6}$$

where $P_i^{\max}$ is the generation limit of the i-th DG in the AC subgrid. While for DC DGs is given by.

$$\gamma_{\text{P}} = \begin{cases} 2\,a_i P_i^{\min} + b_i, P_i < P_i^{\min} \\ 2\,a_i P_i + b_i, P_i^{\min} < P_i < P_i^{\max} \\ 2\,a_i P_i^{\max} + b_i, P_i > P_i^{\max} \end{cases} \tag{7}$$

where, $P_i^{\max}$ is the generation limit of the i-th DG in the DC subgrid.

$$\begin{cases} \text{AC subgrid- Local economic operation:} \\ \lambda_{\text{p1}} = \cdots = \lambda_{pi} = \cdots = \lambda_{pn} = \lambda_{ac} \end{cases} \tag{8}$$

$$\begin{cases} \text{DC subgrid- Local economic operation:} \\ \gamma_{\text{p1}} = \cdots = \gamma_{pj} = \cdots = \gamma_{pn} = \gamma_{dc} \end{cases} \tag{9}$$

When the ICs of all AC/DC DGs are the same, global economic operation (GEO) can be attained. Consequently, the TGC will be reduced to meet eq. 10.

$$\lambda_{ac} = \gamma_{dc} \tag{10}$$

C. REACTIVE POWER DISPATCH

Since the TGC of AC DGs is influenced by both the active and reactive power supplied, optimizing reactive power within the AC subgrid becomes crucial. To achieve this objective, as the active power IC's concept explained in Section II-B above, the total cost and the RMC are in eq. 11 and 12 are presented

to reduce the generation of reactive power in distributed manner, where Q_i and S_i are the reactive and apparent power capacity of AC_{DGi}, respectively i.e., $S_i = \frac{S_{i-\max} - S_i}{S_{i-\max}}$ [34].

$$C(Q_i) = a_i S_i Q_i^2 + b_i Q_i + c_i \tag{11}$$

$$\phi_Q = \frac{dC(Q_i)}{dQ_i} = 2a_i S_i Q_i + b_i \tag{12}$$

The cost coefficients a_i and b_i depends on the parameters presented in section II-B. To achieve optimal reactive power dispatch for AC DGs, it is imperative that they attain uniform RMC, denoted as: $\phi_{Q1} = \phi_{Qi} = \phi_{Qj}$.

III. OPTIMAL CONTROL FOR AC MICROGRID

A. PRIMARY CONTROL

Droop-based control is adopted for the AC DG's primary control level in AC MG. The droop equations are written as:

$$\omega = \omega^* - k_{dp}(P - P_{refi}), \tag{13}$$

here, ω is the frequency while k_{dp} is droop coefficient, and P is active power. Additionally, the reference power denoted by P_{refi}, which comes from the secondary controller. Furthermore, the reactive power is expressed as follows and makes use of the V/Q droop:

$$E = V_{isec} - k_{dq}\phi_Q. \tag{14}$$

Here, E is the voltage's amplitude, k_{dq} is the coefficient for droop, and ϕ_Q is the RMC. V_{isec} is the secondary reference signal.

B. SECONDARY CONTROL

1) FOR IC CONSENSUS IN AC SUBGRID

The goal of the coordination strategy is to acheive equal IC, which is accomplished using the consensus algorithm below.

$$\begin{cases} \lambda_{refi} = \lambda_{(i)} + \zeta \sum_{j=1}^{n} -l_{(i,j)}\lambda_{(j)}(t), \\ P_{refi} = \dfrac{\lambda_{iref} - \beta_i}{2\alpha_i}. \end{cases} \tag{15}$$

where $\lambda_{(j)} = 2a_i P_i + b_i$. Here $\lambda_{(j)}$ is the index for IC proportion while λ_{ref} and P_{refi} are the optimal IC and optimal power generated by DGi. Moreover, k denotes the time step, and l_{ij} is the j^{th} row and jth column element of the laplacian matrix L. Also, ζ is a scalar number for tuning.

Now given the limitations on power generation, the distributed algorithm for ED is outlined as follows.

$$\begin{cases} \lambda_{refi} = \lambda_{(i)} + \zeta \sum_{j=1}^{n} -l_{(i,j)}\lambda_{(j)}(t), \\ P_{refi} = \begin{cases} P_{imin}, & \lambda_i(k+1) < \lambda_{imin}, \\ \dfrac{\lambda_{refi} - \beta_i}{2\alpha_i}, & \lambda_{imin} \le \lambda_r efi \le \lambda_{imax}, \\ P_{imax}, & \lambda_{refi} > \lambda_{imax}, \end{cases} \end{cases} \tag{16}$$

where $\lambda_{imin} = 2\alpha_i p_{imin} + \beta_i$ and $\lambda_{imax} = 2\alpha_i p_{imax} + \beta_i$ for all $i = 1, 2, \ldots, n$.

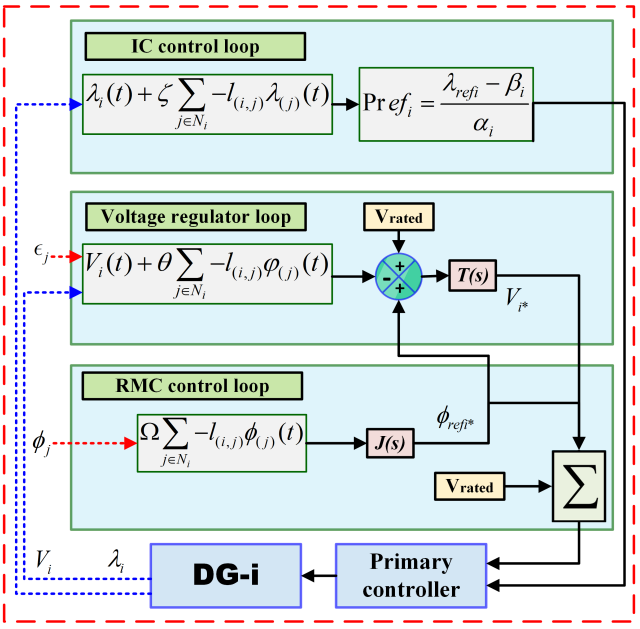

FIGURE 2. Optimal control for AC DGs in AC MG..

2) FOR RMC AND VOLTAGE BALANCING

The other objectives of the coordination technique are voltage regulation and RMC, which are accomplished by applying the consensus strategy below.

$$\phi_{refi} = \Omega \sum_{j=1}^{n} -l_{(i,j)}\phi_{(j)}(t), \tag{17}$$

where $\phi_{(j)} = 2a_i S_{i^*} Q_i + b_i$. Here $\phi_{(j)}$ is index for RMC while ϕ_{ref} is the reference for RMC of DGi.

$$S_{i^*} = \frac{S_{i-\max} - S_i}{S_{i-\max}}$$

Also,

$$V_{refi}(t) = V_i(t) + \mu \sum_{j=1}^{n} -l_{(i,j)}\varphi_{(j)}(t), \tag{18}$$

where $\varphi_{(j)} = \frac{V_i - V_{\min}}{V_{\max} - V_{\min}}$. While, $\varphi_{(j)}$ is the voltage sharing index. V_i is the output voltage. So,

$$V_{i^*}(t) = \left(V_{\text{rated}} - V_{iref}(t) + \phi_{refi^*}\right)\left(k_{vp} - \frac{k_{vi}}{s}\right), \tag{19}$$

where, $\phi_{refi^*} = \phi_{refi} N(s)$ is the compensating signal for RMC k_{vp} and k_{vi} are the terms of the PI controller M(s). $V_{i^*}(k)$ is the compensating signal for voltage regulation. Finally,

$$V_{isec}(t) = V_{\text{rated}} + \phi_{refi^*} + V_{i^*}(t). \tag{20}$$

Here $V_{isec}(t)$ is the control reference for voltage of DGi. Where ϕ_i^* and $V_{i^*}(t)$ are the compensating signals for the RMC and voltage regulation. The reference (V_{isec}) is generated and sent to the primary controller. The comprehensive control for AC DGs is shown in Fig. 2.

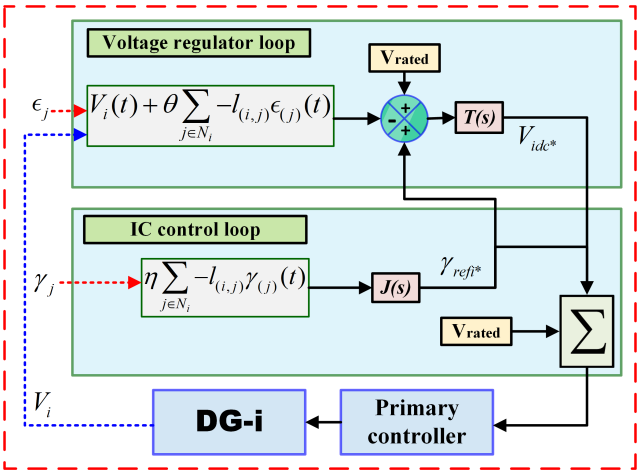

FIGURE 3. Optimal control for DC DGs in DC MG.

IV. OPTIMAL CONTROL FOR DC MICROGRID

A. PRIMARY CONTROL

Droop control is utilized in DC microgrid and is presented as follow.

$$V = V_{ref} - m\gamma_{dc}, \tag{21}$$

here, V is the output voltage while m is for droop coefficient and γ_{dc} for the measured IC. Also, V_{ref} is the secondary reference signal.

The droop coefficient can be written in the form of maximum available power from the converter $P_{\max}$ and the maximum voltage drop ΔV, as shown in 22.

$$\frac{\Delta V}{P_{\max}}. \tag{22}$$

B. SECONDARY CONTROL

The control objectives for the DC MG, 1) achieving average voltage restoration and 2) economic dispatch, are described as follows.

$$\lim_{t\to T}\left|\frac{1}{n}\sum_{i=1}^{n} v_i - v_{ref}\right| = V_{rated} \quad \forall t \geq T, \tag{23}$$

$$\lim_{t\to T}\left|\gamma_i - \gamma_j\right| = 0 \quad \forall t \geq T, \tag{24}$$

here, T is the settling time limit.

The proposed voltage consensus control is given below.

$$V_{\text{iSec-ref}} = V_i(t) + \theta\sum_{j=1}^{n} -l_{(i,j)}\varepsilon_{(j)}(t). \tag{25}$$

where $\varepsilon_{(j)} = \frac{V_i - V_{\min}}{V_{\max} - V_{\min}}$. Here, $\varepsilon_{(j)}$ is the voltage sharing index. The DC economic dispatch can be attained by regulating the IC of the DGs. The power loop is designed to balance the IC of DGs and the control input of the power control loop for DG_i is formulated according to the deviation of its IC.

The output of the proposed IC based secondary controller is shown in 25.

$$\gamma_{refi} = \eta\sum_{j=1}^{n} -l_{(i,j)}\gamma_{(j)}(k), \tag{26}$$

where $\gamma_{(j)} = 2a_iP_i + b_i$. Here $\gamma_{(j)}$ is the IC index while η is a positive scalar number for convergence. While the generating constraints are given as.

$$\lambda_i^* = \begin{cases} \lambda_{imax} & \text{if } (\lambda_i > \lambda_i^{\max}) \\ \lambda_{imin} & \text{if } (\lambda_i < \lambda_i^{\min}) \\ \lambda_i, & \text{others} \end{cases} \tag{27}$$

Also,

$$\gamma_{refi^*}(t) = \gamma_{refi}J(s), \tag{28}$$

here $\gamma_{refi^*}(t)$ is the compensatory IC signal. $C(s)$ is the PI controller. Now from figure 3,

$$V_{i-dc^*}(t) = \left(V_{\text{rated}} - V_{iSec\text{-}ref} + \gamma_{refi^*}(t)\right)(\text{T(s)}). \tag{29}$$

here T(s) is the PI controller. From eq. 28 and 29 we have:

$$V_{\text{ref}} = V_{\text{rated}} + V_{i-dc^*}(k) + \gamma_{refi^*}(t). \tag{30}$$

where $V_{i-dc^*}(k)$ and $\gamma_{i^*}(t)$ are the compensating signals for the voltage regulation and IC. The reference signal V_{ref} is sent to the primary control. The comprehensive control for DC DGs in DC MG is depicted in Fig. 3.

C. ECONOMIC POWER INTERACTION AMONG AC/DC MGs

1) SINGLE BIC

Our primary focus here is on the power interaction between AC/DC subgrids facilitated by BICs. The incremental cost of all AC/DC DGs in the two MGs must be equal to attain the HMG's overall optimal economic operation. BICs oversee the power transfer among the MGs, thereby adjusting the total power generation in both subgrids and balancing their incremental costs. A practical approach to ensure $\lambda_{ac} = \gamma_{dc}$ involves feeding their difference into a PI controller. The PI controller dictates the interaction of power among the two MGs. By modulating the interaction of power, the total power generation in both subgrids can be adjusted, subsequently influencing their incremental costs to attain equality. For this purpose, λ_{ac} and γ_{dc} are acquired by the BIC via communication links and transmitted to the BIC controller. This transmission is achieved using a PI controller.

$$P_{BIC} = \left(k_{pp} - \frac{k_{pi}}{s}\right)(\lambda_{ac} - \gamma_{dc}), \tag{31}$$

where k_{pp} and k_{pi} are the respective terms of the PI controller D(s).

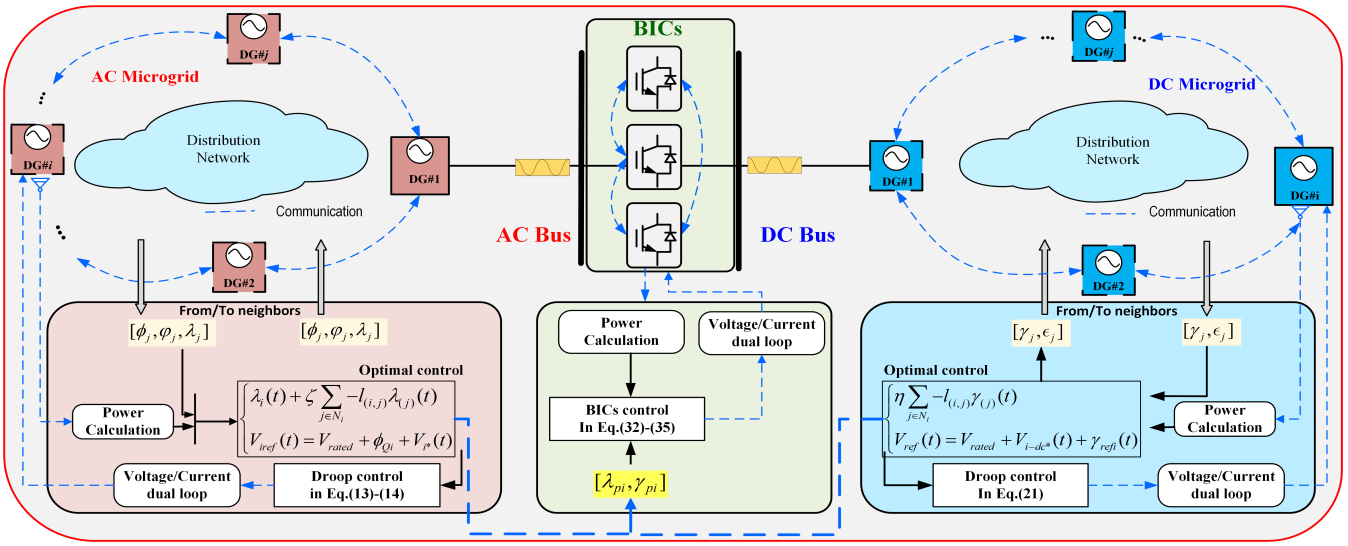

FIGURE 4. Overall control for HMG.

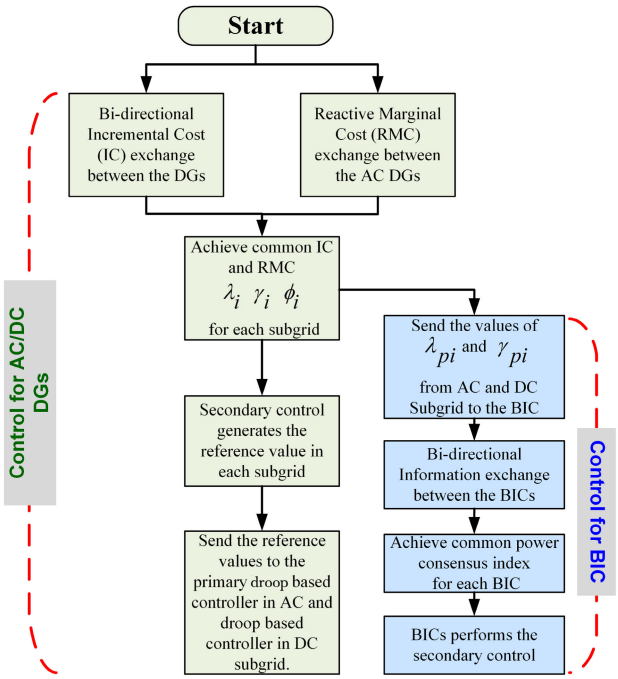

FIGURE 5. Flow of overall control for HMG.

2) MULTIPLE BICs

The goal of the coordination strategy for BICs is to achieve consistent incremental costs for all AC/DC DGs in HMG and to facilitate power transfer among the BICs according to their individual power capacities. The strategy also aims to sustain uniform load factors in order to mitigate the risk of overload in any of the BICs. Therefore, We propose the distributed control based on the communication of BICs as:

$$\varrho_{P-refi} = \kappa \sum_{j=1}^{n} -l_{(i,j)}\delta_{p(j)}(t), \tag{32}$$

where

$$\delta_{p(j)} = \frac{P_{\mathrm{j}}}{P_{\mathrm{nj}}}$$

while $\lambda_{p(j)}$ is the consensus index or normalization index, which denotes the BICs load proportion and can be said to be the load factor of BICs. ϱ_{P-refi} is the control reference of i^{th} BIC. Now based on the eq. 32 from subsection (C(1)) we can write it for multiple BICs as:

$$\Delta P_{BIC} = \left(k_{pp} - \frac{k_{pi}}{s}\right) e_{BIC,j}, \tag{33}$$

where,

$$e_{BIC,j} = \tau(\lambda_{pi} - \gamma_{pi}) + \nu(\varrho_{P-refi}) \tag{34}$$

$$e_{BIC,j} = \tau(\lambda_{pi} - \gamma_{pi}) + \nu(\kappa \sum_{j=1}^{n} -l_{(i,j)}\delta_{p(j)}(t)), \tag{35}$$

here τ and ν are positive coefficients associated with global IC consensus. While the right hand term $e_{BIC,j}$ represents the error in power sharing between BICs, which will diminish to zero as the HMG approaches in steady state. Also, the first term will go to zero due to the PI controller when the ϱ_{P-ref} terms converge to zero.

The overall control for multiple BICs can be seen in Fig. 4. Also, the flowchart of the overall distributed coordination-based economic dispatch with multiple BICs is shown in Fig.5. The IC control signals λ_{pi} and γ_{pi} from the secondary control of AC/DC sub-grids are communicated to the BICs. Using that, the BICs perform the coordination strategy, and thus, the goal of distributed coordination-based economic dispatch is achieved.

V. RESULTS AND DISCUSSION

To assess the performance of the suggested control technique, the HMG with parameters outlined in Table 2 was simulated. The simulated system comprises nine units: 3 AC DGs, 3 DC

TABLE 2. Parameters for AC/DC MGs and BICS.

For AC Subgrid		
DG1	**DG2**	**DG3**
Pn = 6 kW	Pn = 10 kW	Pn = 14 kW
Vn = 311 V	Vn = 311 V	Vn = 311 V
f = 50 Hz	f = 50 Hz	f = 50 Hz
$R_{Lac1} = 0.1 + j3e^{-3}$	$R_{Lac2} = 0.1 + j3e^{-3}$	$R_{Lac3} = 0.1 + j3e^{-3}$
For DC Subgrid		
DG1	**DG2**	**DG3**
$R_{ddc1} = 0.3$Ohm	$R_{ddc2} = 0.5$Ohm	$R_{dc2} = 0.8$Ohm
Pn = 5 kW	Pn = 6 kW	Pn = 8 kW
Kn = 400 V	Vn = 400 V	Vn = 400 V
For BICs		
BIC1	**BIC2**	**BIC3**
Pn = 3 kW	Pa = 4 kW	Pn = 5 kW
$R_1 = 0.025$	$R_2 = 0.025$	$R_3 = 0.025$
$R_{L1} = 1e^{-1} + j2e^{-3}$	$R_{L2} = 1e^{-1} + j2e^{-3}$	$R_{L3} = 1e^{-1} + j2e^{-3}$

TABLE 3. Parameters for AC/DC MGs for all case scenarios.

For all case scenarios		
For AC Subgrid		
DG1	**DG2**	**DG3**
$P_{max} = 6kW$	$P_{max} = 10kW$	$P_{max} = 14kW$
$P_{min} = 0kW$	$P_{min} = 0kW$	$P_{min} = 0kW$
$a_1 = 1.2e^{-2}$	$a_2 = 1.5e^{-2}$	$a_3 = 1.8e^{-2}$
$b_1 = 5.19e^{-1}$	$b_2 = 5.20e^{-1}$	$b_3 = 5.21e^{-1}$
$c_1 = 10$	$c_2 = 12$	$c_3 = 14$
$\zeta = 1e^{-}2$	$\zeta = 1e^{-}2$	$\zeta = 1e^{-}2$
$\Omega = 1e^{-}1$	$\Omega = 1e^{-}1$	$\Omega = 1e^{-}1$
$\mu = 5e^{-}1$	$\mu = 5e^{-}1$	$\mu = 5e^{-}1$
For DC Subgrid		
DG1	**DG2**	**DG3**
$P_{max} = 5kW$	$P_{max} = 6kW$	$P_{max} = 8kW$
$P_{min} = 0kW$	$P_{min} = 0kW$	$P_{min} = 0kW$
$a_1 = 1.9e^{-2}$	$a_2 = 2.3e^{-2}$	$a_3 = 2.7e^{-2}$
$b_1 = 5.52e^{-1}$	$b_2 = 5.525e^{-1}$	$b_3 = 5.529e^{-1}$
$c_1 = 18$	$c_2 = 22$	$c_3 = 26$
$\eta = 1e^{1}$	$\eta = 1e^{1}$	$\eta = 1e^{1}$
$\theta = 3e^{-}1$	$\theta = 3e^{-}1$	$\theta = 3e^{-}1$

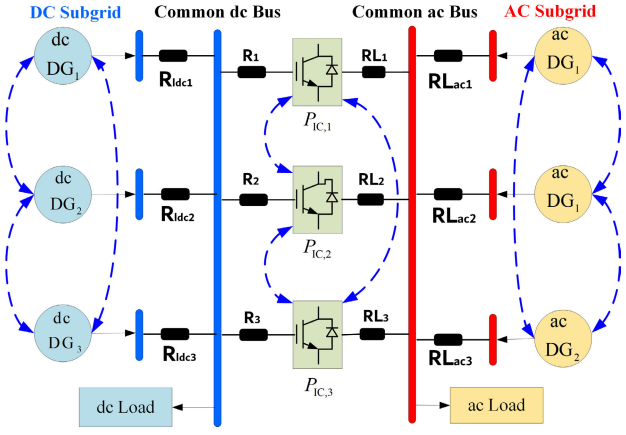

FIGURE 6. Simulated HMG system.

DGs, and three (3) BICs. The cost parameters are listed in Table 3. The simulated HMG is depicted in Fig. 6.

A. TEST NO. 1: OPERATION TEST

In this scenario, different controller parts are activated successively to emphasize the effect of various terms. The total load of the HMG is 12kW, with 7kW on the AC and 5kW on the DC side, respectively while the reactive load is 5kVAR on the AC side. The outcomes of this test are depicted in Figure 7.

The test initiates with the activation of the inner, primary, and secondary controllers. Concerning the proposed secondary control, only the optimal control within each subgrid, taking into account the operational limit constraints, is enabled. For 0 s $<$ t $<$ 7 s, the DGs operate inside their limits. It is observed that consensus is achieved on both the IC and RMC, and active and reactive power is economically redistributed (refer to Fig. 7b and Fig. 7d). Hence, both active (P) and reactive power (Q) are optimally re-dispatched, taking into account the generation costs of the DGs. The load factors for power-limits constraint of AC/DC DGs are within limits, i.e., 1 (see Fig. 7k for AC and DC DGs load factor). The AC voltage, frequency and DC voltage is properly regulated, (see Fig. 7f and Fig. 7h for AC DGs/bus frequency and voltage while Fig. 7i for DC DGs and bus-voltage). Also, the power transfer by the BICs is zero (see Fig. 7e). The λ_P and γ_P consensus are achieved within each MG (see Fig. 7a). The RMC consensus (ϕ_Q) is achieved and can be seen in Fig. 7c. The load factor is defined here for convenience.

$$P_{LF} = \frac{P_i}{P_n}, \tag{36}$$

where P_{LF} represents the load factor of AC/DC DGs and the BICs. Here P_i is the instantaneous power while P_{ni} is the rated power capacity of the respective AC/DC DGs or BICs.

At $t = 7s$, optimization between every DG and the BICs is enabled, but initially only the BICs control is activated but the BICs consensus objective is still disabled. In order to achieve global economic dispatch, the BICs equalize the ICs on both sub MGs. However, as shown in Fig. 7j, they do not distribute proportionate power to their power capacity, which may result in excess loading in the BICs. The frequency and voltage are regulated (see Fig. 7f and Fig. 7h for AC DGs/bus frequency and voltage while Fig. 7i for DC DGs and bus-voltage). As can be shown in Fig. 7j at $t = 13s$, all participating BICs transfer power proportionate to their rated power when the proposed control for BICs is enabled at $t = 13s$. In this scenario, all the BICs and DGs are working within their power limits. The summary of the operation test no. 1 is given in Table 4.

B. TEST 2: LOAD-STEPS

The effectiveness of the suggested strategy in relation to load steps is now examined. The same system (Hybrid AC/DC microgrid) that was utilized in the prior test, with the parameters and adjacency matrix (communication network) remaining the same. The HMG's starting total load (12 kW-7 kW on the AC side and 5 kW on the DC side) is the same as it was in the prior test. The outcomes are displayed in Figure 8. All of the controls and the power limit constraints are turned on at the start of the simulation, meaning that the HMG is fully optimized. The DGs are attaining λ_P and γ_P

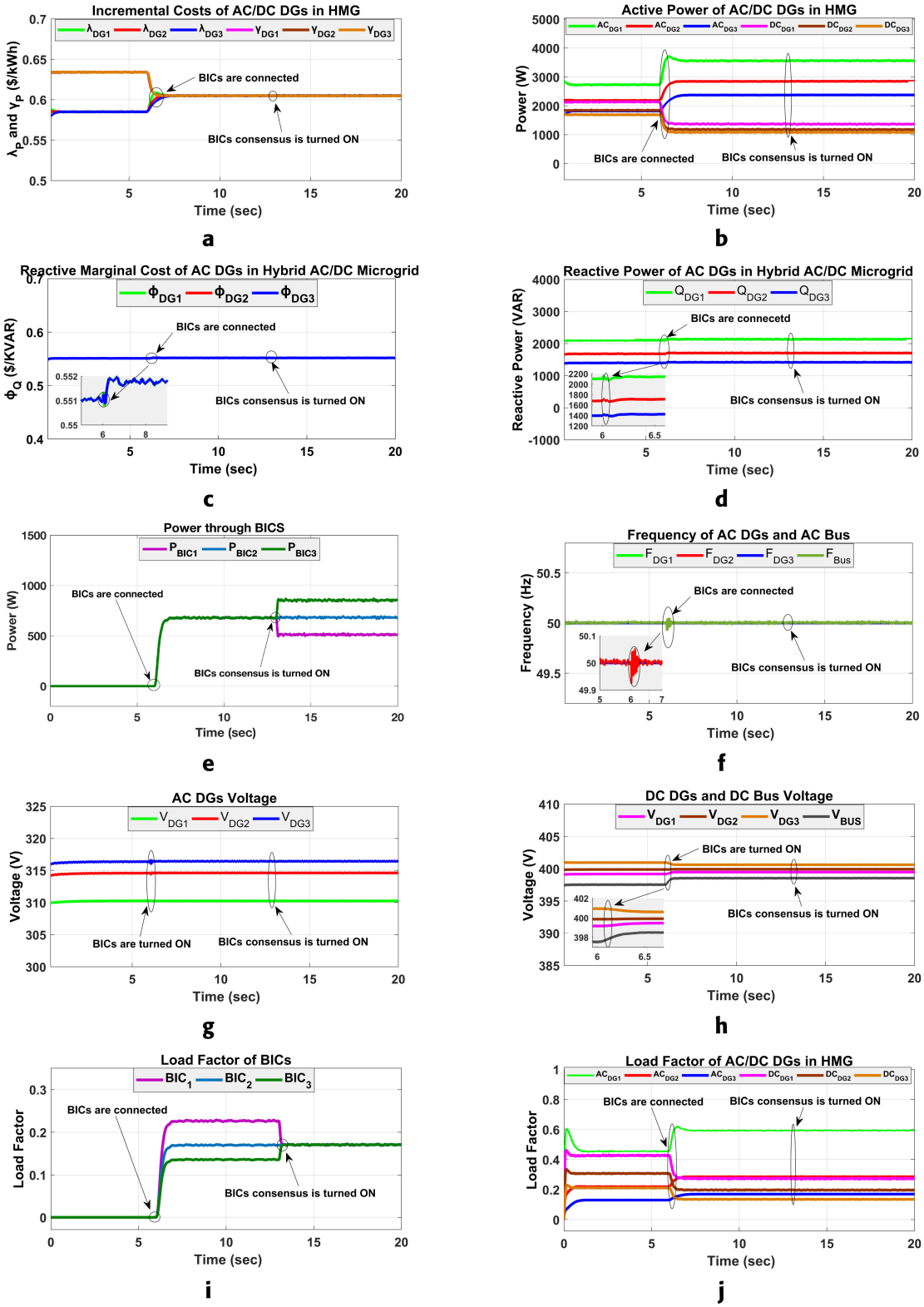

FIGURE 7. Case 1: Operation Test:(a) Incremental costs of AC and DC DGs, (b) Active power of Ac and DC DGs, (c) RMC for AC DGs, d) Reactive power of AC DGs, (e) Power for BICs, (f) AC DGs and bus frequency, and (g) Voltage of AC DGs, (h) DC DGs and bus voltage, (i) Load factor of BICs, (j) Load factor of AC and DC DGs.

consensus for 0 s $<$ t $<$ 7 s, while the BICs are obtaining δ_P consensus (see Fig. 8i). The secondary variables (voltage, DC, and AC bus frequency) are regulated as depicted in Fig. 8f, 8g, and 8h.

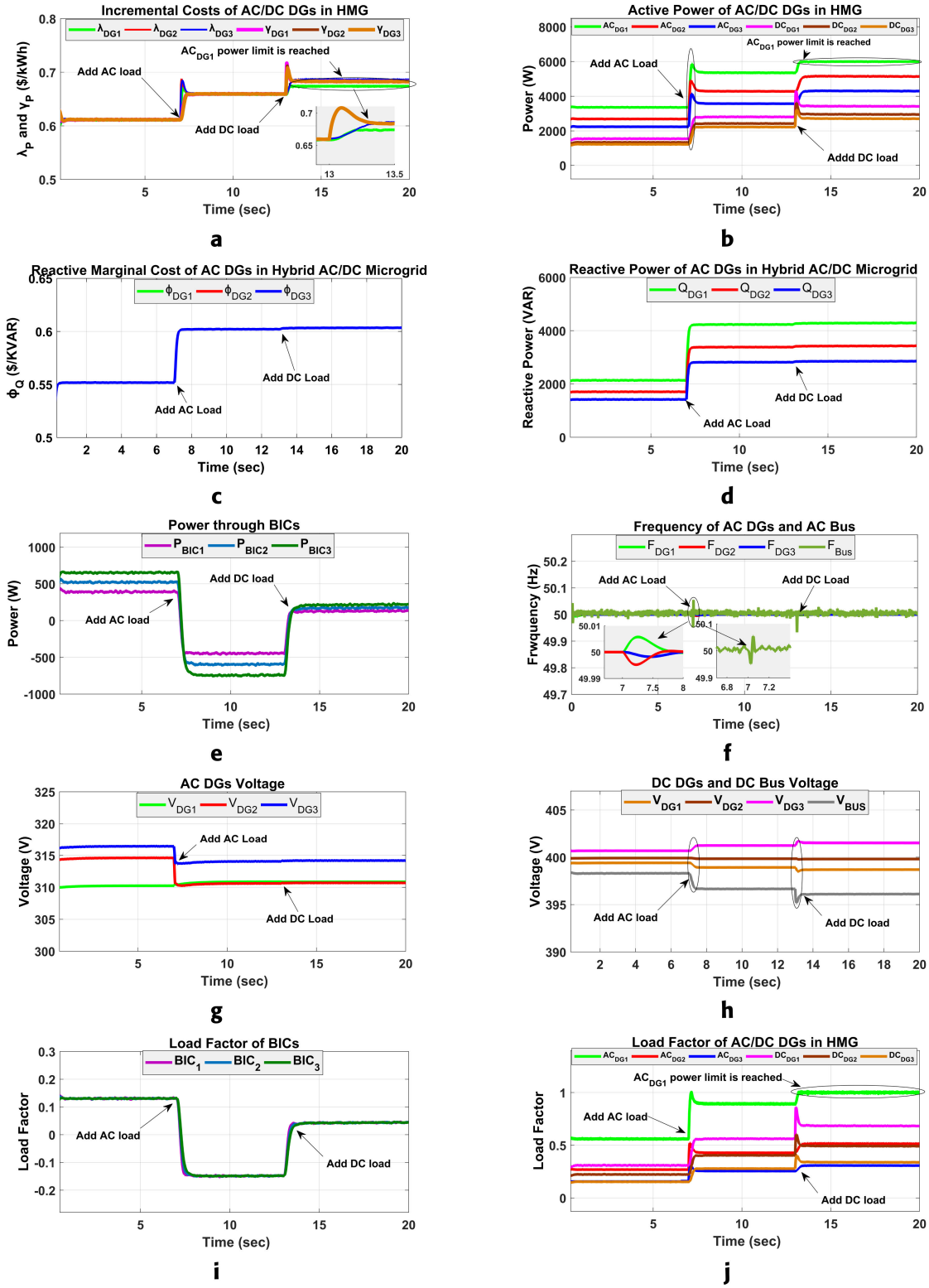

FIGURE 8. Case 2: Load Steps:(a) Incremental costs of AC and DC DGs, (b) Active power of Ac and DC DGs, (c) RMC for AC DGs, d) Reactive power of AC DGs, (e) Power for BICs, (f) AC DGs and bus frequency, and (g) Voltage of AC DGs, (h) DC DGs and bus voltage, (i) Load factor of BICs, (j) Load factor of AC and DC DGs.

At $t = 7s$, a load change is introduced at the AC side and is 9 kW, 5 kVAR. As a result of the load power change, the HMG still achieves the λ_P and γ_P consensus. Moreover, the load factors of AC/DC DGs and the BICs are within the limits (see Fig. 8j and Fig. 8i). The reactive marginal cost consensus λ_Q is also achieved and can be seen in Fig. 8c.

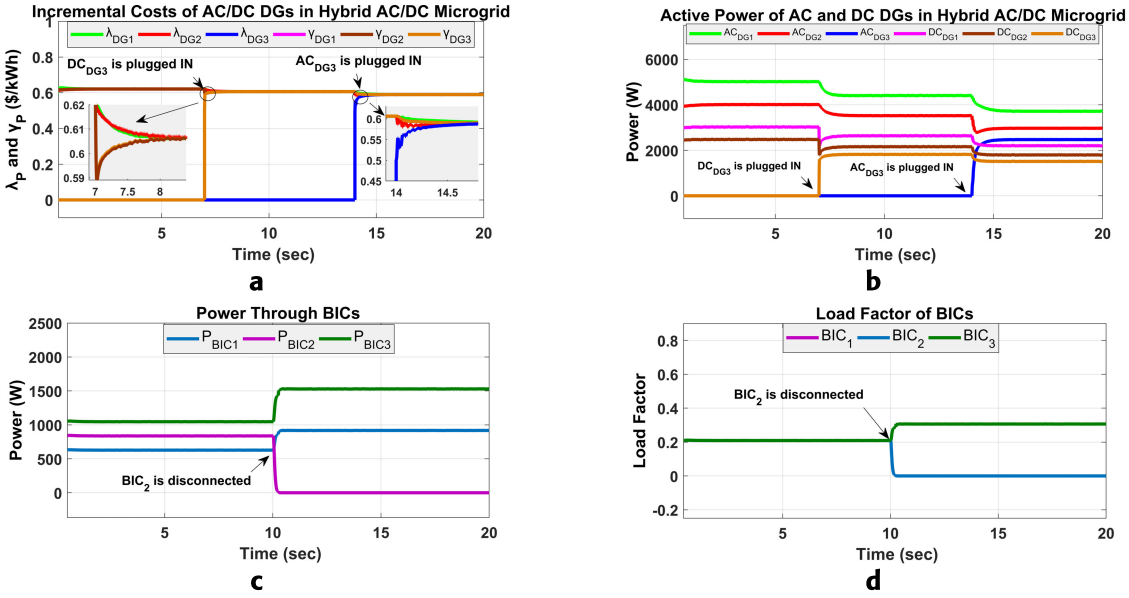

FIGURE 9. Case 3: PnP:(a) Incremental costs of AC and DC DGs, (b) Active power of Ac and DC DGs, (c) Power for BICs, (d) Load factor of BICs.

TABLE 4. Summary for operation test no. 1.

Operating condition	Time	Results
Only optimization within the subgrids (within AC and DC subgrid) is enabled	0 to 7 sec	Both active and reactive (for AC sub-MG only) power are re-dispatched optimally for both sub-grids locally
Optimization among AC/DC subgrids is enabled (BICs control is enabled)	7 to 13 sec	The BICs equalize the ICs on both MGs to attain global ED
Full optimization including BIC consensus is enabled	13 to 20 sec	All the participating BICs transfers proportionate power to their rating

Because AC DGs are less expensive, they may transmit more power via the BICs (see Fig. 8e) and reach the optimal dispatch point (see Fig. 8b). The DGs achieve the IC and RMC consensus, and the secondary variables are constantly regulated.

At $t = 13s$, another load change is introduced at the DC side and is increased by 4 kW. Due to the change in the load, AC_{DG1} reaches its capacity limit i.e., the power limit, and it goes out of the IC consensus. It can be seen in Fig. 8a and Fig. 8b that the AC_{DG1} is out of the IC consensus, but the remaining 5 DGs (2 AC and 3 DC DGs) are still operating and achieving the IC consensus. The load factors of AC/DC DGs and the BICs is shown in Fig. 8j and Fig. 8i. It can be seen in Fig. 8j that the load factor/ power limit of AC_{DG1} is restricted at it's maximum value that is 1. All the other units are operating within their power limits. One more time, the λ_P and γ_P consensus are attained by the DGs (Fig. 8a) and by the BICs (see Fig. 8i).

This case scenario demonstrates the effectiveness of the proposed control strategy in maintaining consensus and regulation under varying load conditions in the HMG. Despite load changes at both the AC and DC sides, the system achieved consensus for primary and secondary variables. The control strategy ensures optimized and stable microgrid performance even with dynamic load variations.

C. TEST 3: PnP

This scenario validates the proposed distributed control's performance in PnP case. The outcomes are displayed in Figure 9. All of the controls and the power limit constraints are turned on at the start of the simulation.

It can be seen from Fig. 9a and Fig. 96 that the AC_{DG3} and DC_{DG3} in the AC/DC subgrids are initially plugged out. The DC_{DG3} is plugged IN at $t = 7s$, and as depicted in Fig. 9a that the IC of the hybrid AC/DC microgrid is decreased; also, the power of AC/DC DGs is decreased. Similarly, at $14s$, the AC_{DG3} is plugged IN, and as depicted in Fig. 9a, the IC of the HMG is decreased further; also, the power of AC and DC DGs is decreased as can be seen in Fig. 9b. Similarly, for the BICs, it can be seen that at $t = 10s$, the BIC 3 is plugged OUT from the system of 3 BICs as depicted in Fig. 9c. The remaining 2 BICs share its power in a way that BICs consensus is still achieved between the remaining two BICs and can be seen in Fig. 9c, while the load factor/ power limits of the BICs are still in their respective limits and can be seen in Fig. 9d.

The proposed control effectively manages PnP scenarios, maintaining system optimization while keeping power limits within constraints.

D. TEST 4: COMPARISON TEST

The suggested control method and the documented method in [35] are contrasted in this section. The suggested approach in [35] restores secondary variables to their nominal values

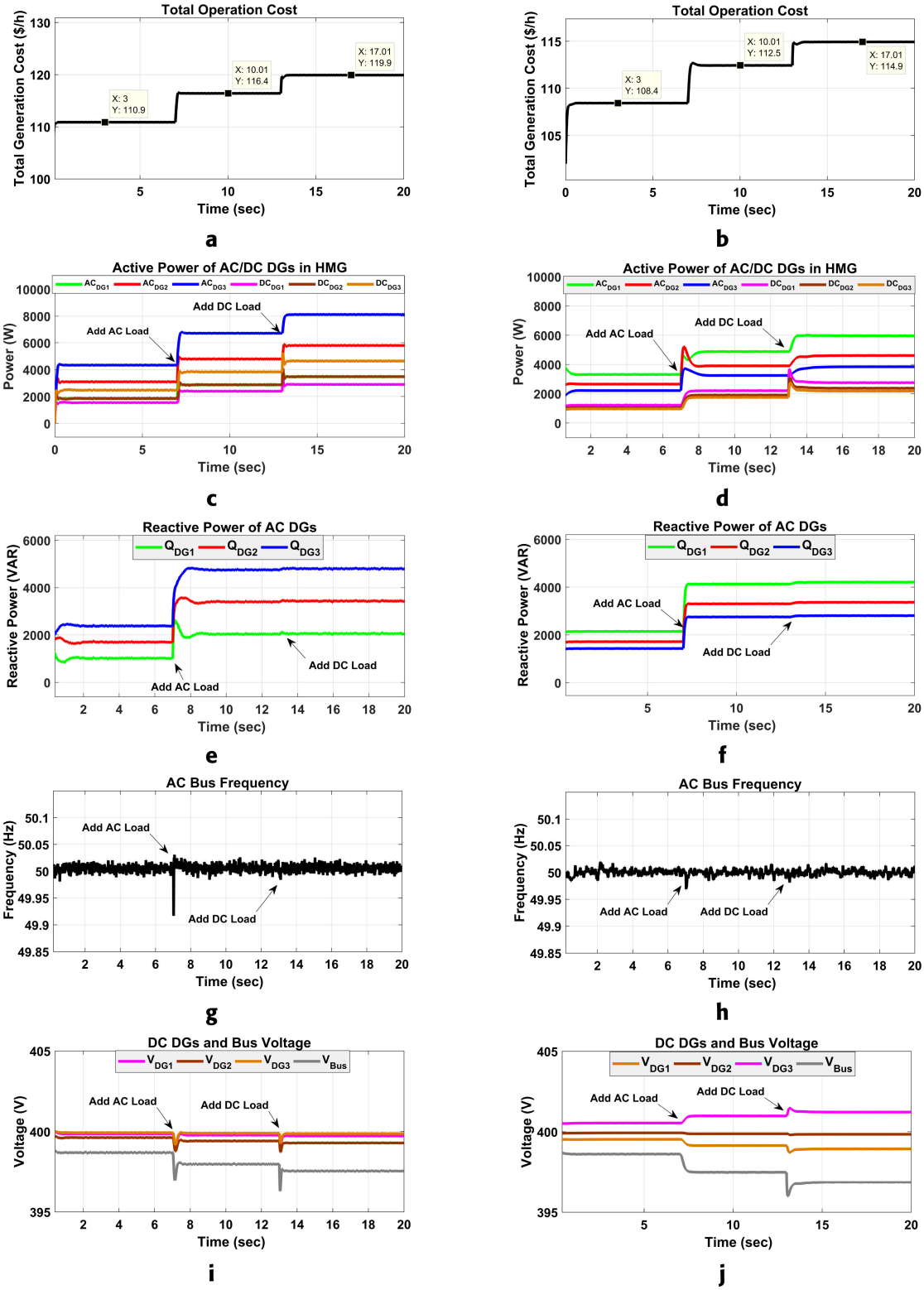

FIGURE 10. Case 4: Comparison test (left side are results with [35] while right hand are results with proposed control:(a)(b) TGC of hybrid AC/DC microgrid, (c)(d) Active power of AC and DC DGs, (e)(f) Reactive power of AC DGs, (g)(h) AC bus frequency, (i)(j) DC DGs and bus voltage.

while sharing proportionate without taking into account the DGs' generating costs. Both the suggested control and the control in [35] begin the test with every feature turned ON. The loading condition and load changes in HMG are the same for both strategies: from $t = 0$ to $5s$, the load on the AC side is 7 kW, 5kVAR, while on the DC side is 5 kW. Now, at $t = 7s$,

TABLE 5. Comparison of total generation cost.

Time step (sec)	Proposed Control Cost $\$/h$	Ref. [35] Cost $\$/h$
$t = 0 - 7$	108.4	110.9
$t = 7 - 13$	112.5	116.4
$t = 13 - 20$	114.9	119.9

the load on AC side is increased by 7 kW, 5kVAR, and finally, at $t = 13$, the DC load stepped up by 4 kW.

Fig. 10 illustrates the comparison results for TGC for both control schemes. Now, with full load connected, the TGC is decreased by 4.2%, i.e., from 119.9$\$/h$ to 114.9$\$/h$, as depicted in Fig. 10a and Fig. 10b. Also, Fig. 10c, Fig. 10d, Fig. 10e, and Fig. 10f depicts the results of active of AC/DC DGs and reactive power of AC DGs in HMG for both controls. The active and reactive powers with proposed control are re-dispatched according to their cost where the cheap DG and cheap MG shares more power thereby reducing the total generation cost. In comparison to the control presented in [35], the proposed control reduces the TGC because the power is re-dispatched according to the AC/DC DGs cost i.e., The TGC is reduced from 119.9$\$/h$ to 114.9$\$/h$. Similarly, Fig. 10g, Fig. 10h, Fig. 10i, and Fig. 10j depicts the results for AC bus frequency and DC DGs and bus voltages for both controls. Table 5 shows the comparison of TGC for proposed control and control presented in [35].

The proposed control strategy optimizes power dispatch based on cost, resulting in more efficient power sharing and cost savings. While the cost reduction of 4.2% in TGC may appear modest due to the small scale of the HMG, it could hold a substantial impact in a larger HMG context.

VI. CONCLUSION

This paper introduced a consensus-based distributed secondary control strategy for optimal power dispatch, frequency regulation, and DC voltage control within islanded hybrid AC/DC microgrids. The primary control framework featured local control for AC/DC DGs through droop-based control. Considering power limitations, a secondary control based on a distributed coordination approach is utilized for AC/DC DGs in a HMG. The suggested control successfully achieves AC frequency restoration, DC voltage regulation, and optimal economic operation of both active and reactive marginal costs for all participating AC/DC DGs. Additionally, a distributed active power control method is proposed to manage multiple BICs, ensuring proportional power sharing to prevent overloading. The dynamic performance of the proposed control is rigorously evaluated and addressed under various scenarios, including load changes and PnP. Comparative analysis against existing control techniques validates the strategy's superiority, resulting in a noteworthy reduction of HMG operation costs.

In large-scale microgrids, increasing DGs challenge the scalability of distributed control strategies and pose cyber-security risks like cyber-attacks and network congestion. These are some of the major aspects and points to be considered in the future studies. Our future research will focus on developing efficient distributed optimization algorithms, cyber-attack mitigation strategies, and event-triggered control methods. The authors will validate the proposed control strategy using HIL and RT-Lab testing, with plans for real-time implementation in the future study.

REFERENCES

[1] Y. Wang, S. Mondal, C. Deng, K. Satpathi, Y. Xu, and S. Dasgupta, "Cyber-resilient cooperative control of bidirectional interlinking converters in networked AC/DC microgrids," *IEEE Trans. Ind. Electron.*, vol. 68, no. 10, pp. 9707–9718, Oct. 2021.

[2] S. K. Sahoo, A. K. Sinha, and N. K. Kishore, "Control techniques in AC, DC, and hybrid AC–DC microgrid: A review," *IEEE J. Emerg. Sel. Topics Power Electron.*, vol. 6, no. 2, pp. 738–759, Jun. 2018.

[3] P. Lin, C. Jin, J. Xiao, X. Li, D. Shi, Y. Tang, and P. Wang, "A distributed control architecture for global system economic operation in autonomous hybrid AC/DC microgrids," *IEEE Trans. Smart Grid*, vol. 10, no. 3, pp. 2603–2617, May 2019.

[4] J. M. Guerrero, J. C. Vasquez, J. Matas, L. G. de Vicuna, and M. Castilla, "Hierarchical control of droop-controlled AC and DC microgrids—A general approach toward standardization," *IEEE Trans. Ind. Electron.*, vol. 58, no. 1, pp. 158–172, Jan. 2011.

[5] A. K. Sahoo, K. Mahmud, M. Crittenden, J. Ravishankar, S. Padmanaban, and F. Blaabjerg, "Communication-less primary and secondary control in inverter-interfaced AC microgrid: An overview," *IEEE J. Emerg. Sel. Topics Power Electron.*, vol. 9, no. 5, pp. 5164–5182, Oct. 2021.

[6] G. Qi, A. Chen, and J. Chen, "Improved control strategy of interlinking converters with synchronous generator characteristic in islanded hybrid AC/DC microgrid," *CPSS Trans. Power Electron. Appl.*, vol. 2, no. 2, pp. 149–158, 2017.

[7] J. C. Vasquez, J. M. Guerrero, M. Savaghebi, J. Eloy-Garcia, and R. Teodorescu, "Modeling, analysis, and design of stationary-reference-frame droop-controlled parallel three-phase voltage source inverters," *IEEE Trans. Ind. Electron.*, vol. 60, no. 4, pp. 1271–1280, Apr. 2013.

[8] A. Bidram and A. Davoudi, "Hierarchical structure of microgrids control system," *IEEE Trans. Smart Grid*, vol. 3, no. 4, pp. 1963–1976, Dec. 2012.

[9] R. Babazadeh-Dizaji and M. Hamzeh, "Distributed hierarchical control for optimal power dispatch in multiple DC microgrids," *IEEE Syst. J.*, vol. 14, no. 1, pp. 1015–1023, Mar. 2020.

[10] M. Zaery, P. Wang, W. Wang, and D. Xu, "Distributed global economical load sharing for a cluster of DC microgrids," *IEEE Trans. Power Syst.*, vol. 35, no. 5, pp. 3410–3420, Sep. 2020.

[11] A. Navas, J. S. Gomez, J. Llanos, E. Rute, D. Saez, and M. Sumner, "Distributed predictive control strategy for frequency restoration of microgrids considering optimal dispatch," *IEEE Trans. Smart Grid*, vol. 12, no. 4, pp. 2748–2759, Jul. 2021.

[12] J. Llanos, D. E. Olivares, J. W. Simpson-Porco, M. Kazerani, and D. Sáez, "A novel distributed control strategy for optimal dispatch of isolated microgrids considering congestion," *IEEE Trans. Smart Grid*, vol. 10, no. 6, pp. 6595–6606, Nov. 2019.

[13] Z. Li, Z. Cheng, J. Si, and S. Li, "Distributed event-triggered hierarchical control to improve economic operation of hybrid AC/DC microgrids," *IEEE Trans. Power Syst.*, vol. 37, no. 5, pp. 3653–3668, Sep. 2022.

[14] F. Nejabatkhah and Y. W. Li, "Overview of power management strategies of hybrid AC/DC microgrid," *IEEE Trans. Power Electron.*, vol. 30, no. 12, pp. 7072–7089, Dec. 2015.

[15] E. Espina, J. Llanos, C. Burgos-Mellado, R. Cárdenas-Dobson, M. Martínez-Gómez, and D. Sáez, "Distributed control strategies for microgrids: An overview," *IEEE Access*, vol. 8, pp. 193412–193448, 2020.

[16] Q. Zhou, M. Shahidehpour, A. Paaso, S. Bahramirad, A. Alabdulwahab, and A. Abusorrah, "Distributed control and communication strategies in networked microgrids," *IEEE Commun. Surveys Tuts.*, vol. 22, no. 4, pp. 2586–2633, 4th Quart., 2020.

[17] F. Chen, M. Chen, Q. Li, K. Meng, Y. Zheng, J. M. Guerrero, and D. Abbott, "Cost-based droop schemes for economic dispatch in islanded microgrids," *IEEE Trans. Smart Grid*, vol. 8, no. 1, pp. 63–74, Jan. 2017.

[18] Y. Lan, X. Guan, and J. Wu, "Online decentralized and cooperative dispatch for multi-microgrids," *IEEE Trans. Autom. Sci. Eng.*, vol. 17, no. 1, pp. 450–462, Jan. 2020.

[19] P. Buduma, M. K. Das, S. Mishra, and G. Panda, "Robust power management and control for hybrid AC-DC microgrid," in *Proc. 3rd Int. Conf. Energy, Power Environ., Towards Clean Energy Technol.*, Mar. 2021, pp. 1–6.
[20] W. Feng, J. Yang, Z. Liu, H. Wang, M. Su, and X. Zhang, "A unified distributed control scheme on cost optimization for hybrid AC/DC microgrid," in *Proc. IEEE 4th Southern Power Electron. Conf. (SPEC)*, Dec. 2018, pp. 1–6.
[21] J. Zhao and F. Dörfler, "Distributed control and optimization in DC microgrids," *Automatica*, vol. 61, pp. 18–26, Nov. 2015.
[22] S. H. Hanzaei, M. Korki, and X.-M. Zhang, "Distributed cooperative voltage mode control for DC-isolated microgrids powered by renewable energy sources," *Int. J. Electr. Power Energy Syst.*, vol. 152, Oct. 2023, Art. no. 109175, doi: 10.1016/j.ijepes.2023.109175.
[23] R. de Azevedo, M. H. Cintuglu, T. Ma, and O. A. Mohammed, "Multiagent-based optimal microgrid control using fully distributed diffusion strategy," *IEEE Trans. Smart Grid*, vol. 8, no. 4, pp. 1997–2008, Jul. 2017.
[24] F. Dörfler, J. W. Simpson-Porco, and F. Bullo, "Breaking the hierarchy: Distributed control and economic optimality in microgrids," *IEEE Trans. Control Netw. Syst.*, vol. 3, no. 3, pp. 241–253, Sep. 2016.
[25] M. Salman, Y. Li, and J. Xiang, "A consensus index-based distributed control for islanded AC microgrids," in *Proc. IEEE 7th Conf. Energy Internet Energy Syst. Integr. (EI)*, Hangzhou, China, Dec. 2023, pp. 2365–2370, doi: 10.1109/EI259745.2023.10512684.
[26] Y. Cao, X. Pan, and Y. Sun, "Dynamic economic dispatch of AC/DC hybrid microgrid based on consensus algorithm," in *Proc. IEEE 3rd Conf. Energy Internet Energy Syst. Integr. (EI)*, Nov. 2019, pp. 319–324.
[27] L. Li, X. Bai, Y. Guo, J. Zhang, C. Chen, Y. Yi, and A. Wang, "Distributed optimal dispatching of AC/DC hybrid microgrid based on consensus algorithm," in *Proc. 6th Asia Conf. Power Electr. Eng. (ACPEE)*, Apr. 2021, pp. 1398–1402.
[28] B. Papari, G. Ozkan, H. P. Hoang, P. R. Badr, C. S. Edrington, H. Parvaneh, and R. Cox, "Distributed control in hybrid AC-DC microgrids based on a hybrid MCSA-ADMM algorithm," *IEEE Open J. Ind. Appl.*, vol. 2, pp. 121–130, 2021.
[29] F. Wang, Y. Li, and Z. Zhang, "Cooperative control of hybrid microgrids: An economic dispatch solution," in *Proc. 2nd Int. Conf. Electr. Eng. Mechatronics Technol. (ICEEMT)*, Jul. 2022, pp. 209–213.
[30] W. Cai, S. Yang, G. Sun, Q. Zhang, and H. Yu, "Adaptive load balancing for parameter servers in distributed machine learning over heterogeneous networks," *ZTE Commun.*, vol. 21, no. 1, pp. 72–80, Mar. 2023, doi: 10.12142/ZTECOM.202301009.
[31] M. Salman, Y. Ling, Y. Li, and J. Xiang, "Coordination-based power management strategy for hybrid AC/DC microgrid," *IEEE Syst. J.*, vol. 17, no. 4, pp. 6528–6539, Dec. 2023, doi: 10.1109/JSYST.2023.3315795.
[32] E. Rute-Luengo, A. Navas-Fonseca, J. S. Gómez, E. Espina, C. Burgos-Mellado, D. Sáez, M. Sumner, and D. Muñoz-Carpintero, "Distributed model-based predictive secondary control for hybrid AC/DC microgrids," *IEEE J. Emerg. Sel. Topics Power Electron.*, vol. 11, no. 1, pp. 627–642, Feb. 2023.
[33] S. Zheng, K. Liao, J. Yang, and Z. He, "Droop-based consensus control scheme for economic dispatch in islanded microgrids," *IET Gener., Transmiss. Distribution*, vol. 14, no. 20, pp. 4529–4538, Oct. 2020.
[34] A. Navas-Fonseca, C. Burgos-Mellado, J. S. Gómez, E. Espina, J. Llanos, D. Saez, M. Sumner, and D. E. Olivares, "Distributed predictive secondary control with soft constraints for optimal dispatch in hybrid AC/DC microgrids," *IEEE Trans. Smart Grid*, vol. 14, no. 6, pp. 4204–4218, Nov. 2023.
[35] E. Espina, R. Cárdenas-Dobson, J. W. Simpson-Porco, D. Sáez, and M. Kazerani, "A consensus-based secondary control strategy for hybrid AC/DC microgrids with experimental validation," *IEEE Trans. Power Electron.*, vol. 36, no. 5, pp. 5971–5984, May 2021.

MUHAMMAD SALMAN received the B.S. degree in electrical engineering from the University of Engineering and Technology (UET) Peshawar, Pakistan, in 2013, and the M.Sc. degree in electrical engineering (power and control) from COMSATS University, Islamabad, Pakistan, in 2016. He is currently pursuing the Ph.D. degree with the College of Electrical Engineering of Zhejiang University, Hangzhou, China. His research interests include hierarchical control of microgrids, distributed coordination control, power management strategies for hybrid ac/dc microgrids, and application of control related to renewable energy resources.

YANJUN LI received the Ph.D. degree in control science and engineering from Zhejiang University, Hangzhou, China, in 2001. From 2001 to 2003, she was a Postdoctoral Researcher with Zhejiang University and the City University of Hong Kong, Hong Kong. She was an Associate Professor with Zhejiang University, from 2003 to 2008. She is currently a Professor with the School of Information and Electrical Engineering and the Head of the Key Laboratory of Intelligent Systems, Zhejiang University City College, Hangzhou. Her current research interests include complex networks, hybrid and nonlinear systems, system modeling and identification, system optimization, and computational intelligence.

JI XIANG (Senior Member, IEEE) received the Ph.D. degree in control science and engineering from Zhejiang University, Hangzhou, China, in 2005. From 2005 to 2007, he was a Postdoctoral Researcher with Zhejiang University and visited the City University of Hong Kong for three months. Under the support of a Gledden Senior Visiting Fellowship, he visited The University of Western Australia, in 2008. From 2013 to 2014, he was a Visiting Scholar with The University of Sydney, Camperdown, NSW, Australia. He is currently a Professor with the Department of System Science and Engineering, Zhejiang University. His research interests include unman surface vehicle, microgrids, multi agent systems, and complex networks.